Proceedings of the ASME 2017 IMECE International Mechanical Engineering Congress and Exposition
IMECE2017
Nov 3-9, 2017, Tampa, Florida, USA

IMECE2017-71092

DEMONSTRATING THE POTENTIAL OF A NOVEL MODEL TO IMPROVE OPEN-LOOP CONTROL OF ELECTROSTATIC COMB-DRIVE ACTUATORS IN ELECTROLYTES

Ohiremen Dibua
Stanford University Department
of Mechanical Engineering
Stanford, California, USA

Vikram Mukundan
Form Factor Inc,
San Jose, California, USA

Beth Pruitt
Stanford University Department
of Mechanical Engineering
Stanford, California, USA

Ali Mani
Stanford University Department
of Mechanical Engineering
Stanford, California, USA

Gianluca Iaccarino
Stanford University Department
of Mechanical Engineering
Stanford, California, USA

ABSTRACT

Electrostatic comb-drive actuators in electrolytes have many potential applications, including characterizing biological structures. Maximizing the utility of these devices for such applications requires a model capable of accurately predicting their behavior over both micron and submicron scales of displacement. Classic circuit models of these systems assume that the native oxide is a pure dielectric and that the ion concentration of the bulk electrolyte is constant. We propose augmented models that separately address these assumptions, and analyze their ability to predict the displacement of the electrostatic actuators in electrolytic solutions. We find that the model which removes the assumption that the native oxide is a pure dielectric most accurately predicts comb-drive actuator behavior in electrolytes.

NOMENCLATURE

Symbol	Name (units)
α	Device Constant $\left(\frac{m}{V^2}\right)$
C_{Bulk}	Capacitance of Bulk (F)
C_{EDL}	Capacitance of Electric Double Layer (F)
C_{Stern}	Capacitance of Stern Layer
C_{OX}	Capacitance of Oxide Layer (F)
c_0	Nominal Concentration of Bulk Electrolyte (μM)
ε_r	Relative Permittivity of Medium
i	Current Flux $\left(\frac{A}{m^2}\right)$
q	Charge Density on Capacitors $\left(\frac{C}{m^2}\right)$
R_{Bulk}	Bulk Resistance (Ω)
R_{OX}	Oxide Resistance (Ω)
τ_1	Time Constant of Bulk and Oxide (s)
τ_2	Time Constant of Bulk (s)
τ_{OX}	Time Constant of Oxide (s)
V_{Bulk}	Voltage Drop Across Bulk (V)
V_{EDL}	Voltage Drop Across Electric Double Layer (V)
V_{OX}	Voltage Drop Across Oxide (V)
V_{Stern}	Voltage Drop Across Stern Layer (V)
ω	Angular Frequency of AC Signal $\left(\frac{rad}{s}\right)$
Z_{OX}	Impedance of the Oxide Layer (Ω)
Z_{Bulk}	Impedance of the Bulk (Ω)

I. INTRODUCTION

The operation of electrostatic MEMS actuators in air is well understood. The models that exist for these actuators are largely sufficient for predicting their behavior. Over recent years, interest has developed in using electrostatically operated MEMS actuators in conducting liquids. The potential applications of these actuators in electrolytic liquids are mechanically

characterizing biological structures and acting as precisely controlled mechanical parts in microfluidic systems [1]. Work has been done on overcoming the challenges of operating these actuators in electrolytes [1], and on modeling their behavior [2,3]. The previous work focused largely on comb-drive actuators, as does the work in this paper. These models do an excellent job of capturing the pattern of behavior of these actuators as a function of frequency. However, they do not reliably predict both micron and submicron displacements. These previously formulated circuit models assume that the native oxide, which is common to all standardly fabricated MEMS devices, are pure dielectrics and that the ion concentration of the bulk electrolyte is constant. We create models that isolate each of these assumptions. It is shown that creating models that remove both of these assumptions yield improvements in predicting the displacement of electrostatic actuators. It is found that treating the native oxide as a leaky dielectric layer yields the most accurate predictions of actuator displacements.

Here, we present and validate improved models using electrostatic MEMS devices operated in electrolytic solutions. We detail our methodology for model fitting and evaluation of goodness of fit.

II. CURRENT STATE OF THE ART

When analyzing a comb-drive actuator, the overlapping component of the interdigitated finger is viewed as a parallel plate, Figure 1. One set of fingers is fixed, while the other is attached to a spring. The comb-drive actuators are typically operated with DC voltages. In air, this creates a voltage difference between the interdigitated fingers that enables displacement. This changes in electrolytic liquids. In electrolytic liquids, oppositely charged ions coat the electrodes. These ions form two capacitive layers, the stern layer and electric double layer. Most of the DC voltage applied to the system is absorbed by these layers, Figure 2. As a result of this, no displacement occurs in the comb-drive actuator. While challenging, this obstacle is not insurmountable. The stern and electric double layers takes finite time to form. Applying an AC voltage with sufficiently high frequency to the system prevents the formation of these layers. This allows a potential difference to form between the two electrodes, and results in the displacement of the comb-drive actuator [1].

With the method of operation discovered, two papers proposed models to capture the comb-drive behavior in liquid. Mukundan et al. [2] and Panchawagh et al. [3] both did crucial work in constructing a model for this system. Although their models differed in some details of derivation, they essentially took the view of the overlapping regions of the comb-drive as the circuit illustrated in Figure 3. In both papers, it was assumed that the native oxide layer is a pure dielectric with a much smaller capacitance than the stern and electric double layers. As a result, the stern and electric double layers were neglected in the circuit analysis. It was also assumed that the bulk resistor is constant, ie that the concentration of electrolytes in the bulk does not change. In air, the displacement of the comb-drive actuator is modeled as

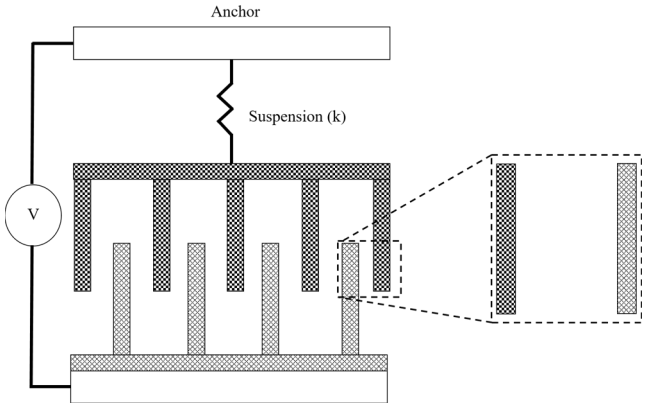

Fig. 1: Illustration of comb-drive actuator and the manner in which a pair of fingers are viewed as parallel plates.

$$x = \varepsilon_r \alpha V^2 \tag{1}$$

where ε_r is the relative permittivity of the medium, V is the voltage difference between two fingers, and α is the device constant, which contains information on the geometry of the comb-drive and the stiffness of the system. When the fingers are immersed in a conducting liquid, two things change in Equation (1). These two things are the relative permittivity, ε_r, and the voltage, V. The voltage that determines the displacement is no longer simply the applied voltage. Instead, it is the voltage across the bulk resistor, V_{Bulk}. This bulk voltage is determined with circuit impedance analysis. Under the assumption that the natural frequency of the device is much smaller than the frequency of the applied sinusoidal voltage, the displacement of the comb-drive actuator in a conducting liquid is determined by

$$x = \varepsilon_r \alpha f(\omega) {V_{Bulk}}^2 = \varepsilon_r \alpha f(\omega) {V_{RMS}}^2 = \varepsilon_r \alpha f(\omega) \left(\frac{V}{\sqrt{2}}\right)^2 \tag{2}$$

where $f(\omega)$ is

$$f(\omega) = \frac{\left(\frac{\omega\tau_1}{2}\right)^2}{1+\left(\omega\left(\frac{\tau_1}{2}+\tau_2\right)\right)^2}. \tag{3}$$

Here, τ_1 is the time constant $R_{Bulk}C_{OX}$ and τ_2 is the time constant $R_{Bulk}C_{Bulk}$. It is assumed that $\tau_1 \gg \tau_2$, since the capacitance of the bulk is much smaller than that of the native oxide.

III. CONSTRUCTION OF NOVEL MODELS

In this section, we outline the creation of two models that remove key assumptions to the model. The first model, the Variable Resistor model, removes the assumption that the resistance of the bulk concentration is constant in time, Figure 4a. The second model, the Leaky Dielectric model, removes the assumption that the native oxide is a pure dielectric, Figure 4b.

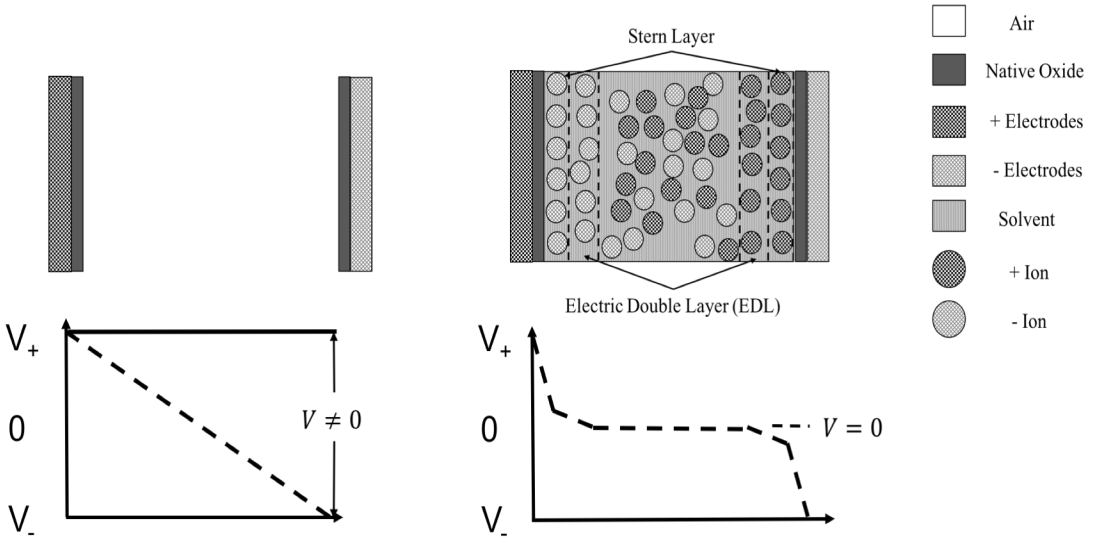

Fig. 2: Drawings of the potential profile between two electrodes when a DC voltage is applied in different mediums. a) In air, the potential profile is linear across the bulk. b) In electrolytes, the Electric Double Layers (EDL) and Stern Layers form. Most of the potential drops across the layers, and none across the bulk.

The variable resistor model is constructed by adding the stern and electric double layers to the classic circuit model. We then make the assumption that the concentration of the bulk electrolyte changes in a spatially homogeneous manner as a function of time. This yields a system of Ordinary Differential Equations (ODEs) of the form

$$\dot{\boldsymbol{y}} = f\big(\boldsymbol{y}, t, V(\omega, t)\big) \tag{4}$$

where $V(\omega, t)$ is the applied sinusoidal voltage at a particular frequency and $\boldsymbol{y}$ is the following vector of states

$$\boldsymbol{y} = [q, V_{OX}, V_{Stern}, V_{EDL}, i, c_0, R_{Bulk}]^T. \tag{5}$$

In Equation (5), $\boldsymbol{q}$ is the charge on the Electric Double Layer (EDL) capacitor, V_{OX} is the voltage drop across the native oxide, V_{Stern} is the voltage drop across the stern layer, V_{EDL} is the voltage drop across the EDL, i is the current, c_0 is the concentration of the bulk electrolyte, and R_{Bulk} is the resistance of the bulk. The detailed state equations are included in Appendix A. We solve (4) for different frequencies, and obtain V_{Bulk} through

$$V_{Bulk}(\omega, t) = iR_{Bulk}(\omega, t). \tag{6}$$

Equation (6) is integrated to obtain

$$V_{RMS}^*(\omega) = \frac{1}{T}\int_0^T V_{Bulk}(\omega, t)^2 dt = g(\omega){V_{RMS}}^2. \tag{7}$$

We note that $g(\omega)$ is not an analytical function of frequency. It is, instead, a numerical function of frequency that is obtained by performing the integral in (7) at different frequencies. Equation (7) is used to rewrite (2) as

$$x = \varepsilon_r \alpha V_{RMS}^*(\omega) = \varepsilon_r \alpha g(\omega){V_{RMS}}^2. \tag{8}$$

The construction of the Leaky Dielectric model is less involved. We perform typical circuit impedance analysis to find the voltage drop across the bulk for the configuration in Figure 4b. This yields

$$x = \varepsilon_r \alpha h(\omega){V_{RMS}}^2. \tag{9}$$

The expression for $h(\omega)$ is given in Appendix B.

IV. ANALYSIS OF NOVEL MODELS

In this section, we discuss how the outputs of the Variable Resistor and Leaky Dielectric models differ from that of the Classic Circuit model.

The Variable Resistor model primarily impacts $V_{Bulk}(\omega, t)$. In the Classic circuit model, V_{Bulk} is always assumed to be a sinusoidal function of time and, as a result, V_{RMS} can be

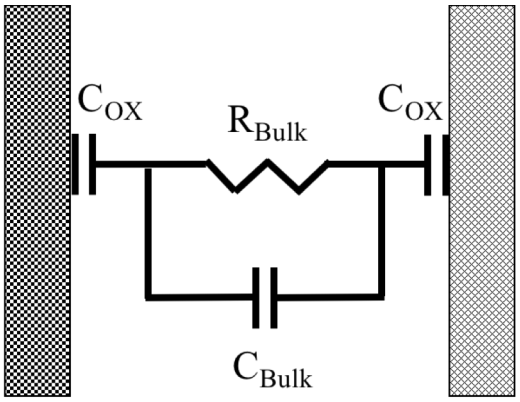

Fig. 3:Circuit representation of a pair of fingers when immersed. in electrolytic liquids, based on the classical circuit model.

calculated analytically. In contrast, the Variable Resistor model produces non-linear bulk voltages at low frequencies. As frequency increases, the bulk voltage becomes a typical sinusoid. An example of a non-sinusoidal bulk voltage at low frequency is illustrated in Figure 5, at a concentration of 100 μM for a *z:z* electrolyte. This results in the relation $V^*_{RMS}(\omega) > f(\omega)V_{RMS}$ for low frequencies when the Classic and Variable Resistor models are fit to the same data. This implies that the Variable Resistor model will predict greater displacements at low frequencies than the Classic Circuit model.

The difference between the Leaky Dielectric and the Classic Circuit models is more fundamental. In the case of the Classic Circuit model, the impedance of the native oxide layer is

$$Z_{OX} = \frac{1}{j\omega C_{OX}} \tag{10}$$

and, in the case of the Leaky Dielectric model, it is

$$Z_{OX} = \frac{R_{OX}}{1+j\omega R_{OX} C_{OX}} \tag{11}$$

We see that, as $\omega \to 0$, $Z_{OX} \to \infty$ in the classic model, while $Z_{OX} \to R_{OX}$ in the Leaky Dielectric model. This difference manifests itself in the limits of $f(\omega)$ and $h(\omega)$ as $\omega \to 0$. Specifically, $f(\omega) \to 0$ and $h(\omega) \to \frac{R_{Bulk}}{2R_{OX}+R_{Bulk}}$. This results in

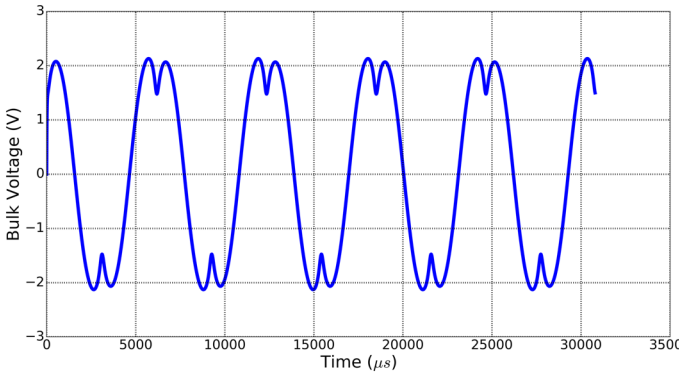

Fig 5: Bulk voltage simulated when the concentration of the z:z electrolyte is 100uM and when the system is subjected to a sinusoidal voltage with an amplitude of 2.6 V and a frequency of 1129Hz.

the Leaky Dielectric model predicting larger displacements at low frequencies than the Classic Circuit model.

Both the Leaky Dielectric and Variable Resistor models imply that the Classic Circuit model underestimates the displacement of the comb-drive actuator at low frequencies. However, these models capture different physics. The relative importance of these physics is evaluated based on the extent to which these models improve our ability to predict the displacement of the comb-drive actuator.

V. EXPERIMENTAL VALIDATION

In this section, we detail fabrication steps for the comb-drive actuator. The devices were created on a silicon-on-insulator (SOI) wafers that have a 15 μm device layer. The relevant features were initially patterned in the silicon through a deep reactive ion etch (DRIE) process. E-beam evaporation was used to deposit a composite metal layer that is made of chromium (Cr

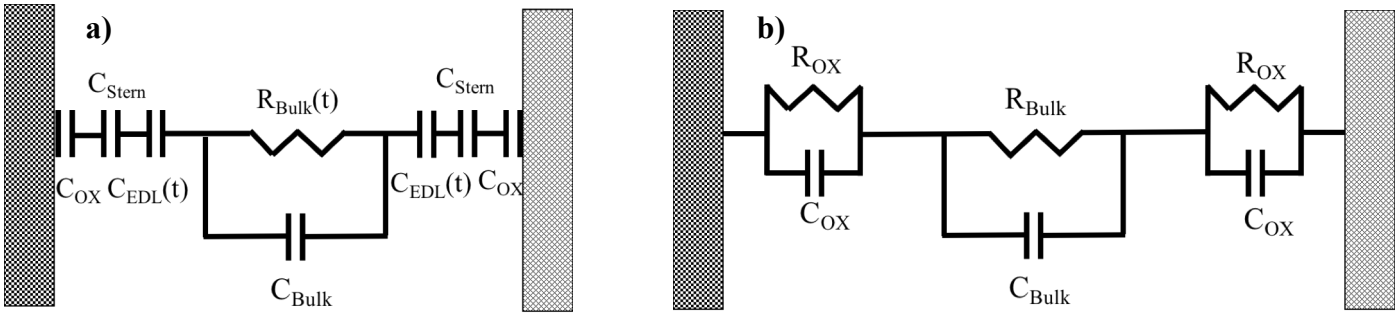

Fig 4: Circuit representation of a pair of fingers when immersed in electrolytic liquids, based on a) the Variable Resistor model, and b) the Leaky Dielectric model.

25 nm)/platinum (Pt 50 nm)/gold (Au 300 nm). The reason gold was used is because it resists corrosion, and, for the purpose of biological experiments, is bio-compatible [2]. Finally, the parylene-C coating was used as a passivation layer for the electrodes [2].

We mount the devices on ceramic dual in-line packages (DIPs), and wire bond them to the DIP with gold wire. Gold wire does not react with electrolytic liquids. Signals that are shifted 90 degrees from one another are applied to the fixed and moving combs, so that there is no attenuation at high frequencies due to parasitic impedances [2]. The signals are applied using a Tektronix AFG 3102C function generator. The device is viewed through a Leica DRMXA2 microscope and the images are taken with a Hamamatsu Digital Camera (C10600).

The following experiment is performed at 100 μM, 500 μM, and 1000 μM concentrations of KCl. A signal with a peak to peak voltage of 5 V is applied at twenty frequencies that are log-spaced from 100 Hz to 1 MHz. The displacement is calculated at each of these frequencies. Fifteen trials of this experiment are performed at each frequency. Figure 6 displays the mean of these displacements. The error bars are representative of two standard deviations of the data.

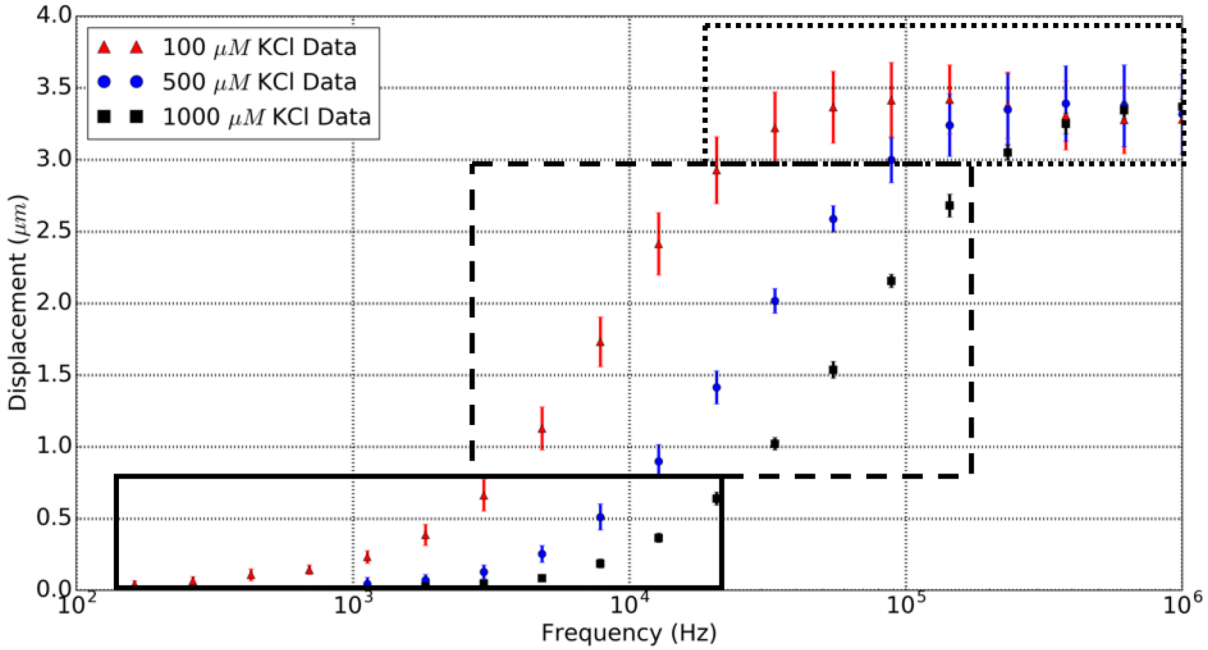

Fig 6: Mean of displacement and error bars that are two standard deviations from the mean at 3 concentrations of KCl. A 5V peak-to-peak signal at frequencies ranging from 100Hz to 1MHz was applied.

VI. MODEL FITTING

We note that the pattern of the measured displacements as a function of frequency is consistent with what is predicted by the Classic Circuit model. At low frequencies, the displacement appears to be relatively constant, followed by a transition into a region of displacement that is linear with respect to frequency on a log-scale. The displacement flattens out at high frequency. These regions are labeled in Figure 6. Finally, the We explain our methods for fitting the three models to data. All of the models are fit using Python's curve_fit function. The curve_fit function implements nonlinear least squares. Our main goal for the data fit, is for the model to have strong predictive power at both micron and submicron displacements. Simultaneously, we do not want data at scales on the same order of magnitude as noise to overtly impact our prediction. With this in mind, we perform a weighted fit such that we disregard all measured displacements that are below 0.1 microns.

The parameters relevant to the Classic Circuit model are easily found using the curve_fit function as described above. The other models require slight modifications to the above procedure. In the case of the Variable Resistor model, multiple initial parameters are fed into the curve_fit function, so that parameters can be estimated that converge to a model output that reasonably fits the data. For the Leaky Dielectric model, it is necessary to require that all of the parameters are greater than zero. Table 1 in the appendix shows the parameters that are used to fit each model to the data. Figure 7 shows the displacements predicted by each model when fit to the data obtained at the three concentrations of KCl. These fits are plotted overtop of the data. Qualitatively, it is seen from the data that both the Leaky Dielectric and Variable Resistor models act as better predictors for the experimental displacement over all relevant ranges of displacement at a concentration of 100 μM. The improvements yielded by the

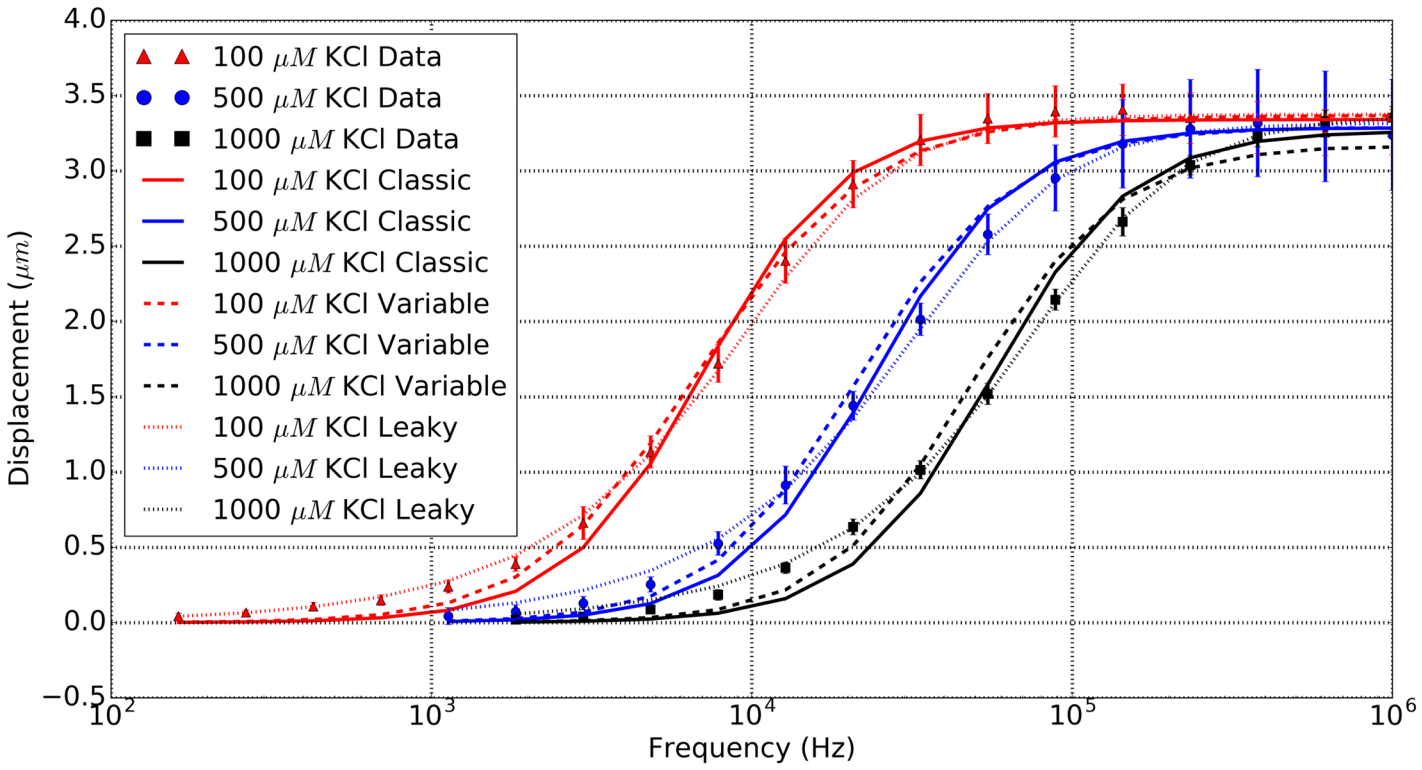

Fig 7: Fits of different models to the data. It is clear that, qualitatively, the Leaky dielectric model appears to fit the data over the entire range of frequency better than the other models at all concentrations.

Variable Resistor model decreases substantially as the concentration increases. This is intuitive since, at larger concentrations, the loss of electrolytes in the bulk should have less of an impact on the system. In contrast, the Leaky Dielectric model appears to yield substantial improvements in predicting displacement across all of the concentrations of KCl used in this experiment.

VII. MODEL EVALUATION

In this section, we evaluate the predictive ability of each model quantitatively. To do so, we use our data, and fitted models in the following way. We first prescribe target displacement values ranging from submicron to micron scale. We then use linear interpolation to find the frequency at which each model achieves these displacements. We then calculate the tracking error of these models by comparing these displacements to the displacements predicted by the data at these frequencies when each trial of the experimental data is interpolated. This results in 15 sets of tracking errors at each target displacement and for each concentration of KCl. Figures 8a-8c shows the resulting mean of the tracking error for each of these three concentrations of KCl. There is sufficient data to obtain reasonable interpolated experimental values, giving us confidence in the value of our calculated tracking errors.

From these plots, it is clear that the Leaky Dielectric model best predicts the displacement of the comb-drive actuator in electrolytic liquids. The Variable Resistor model slightly outperforms the Leaky Dielectric model at submicron scales at a concentration of 100 μM KCl. However, this increased accuracy at submicron scales comes at the cost of accuracy at micron scale displacement. At higher concentrations, the Variable Resistor model outperforms the classic circuit model at low frequencies. As in the 100 μM KCl case, this degrades the performance of the model at high frequencies. At KCl concentrations of 100 μM and 500 μM, the Leaky Dielectric model performs comparably to the Variable Resistor model at low frequencies, and performs substantially better at a concentration of 1000 μM. Unlike the Variable Resistor model, the improved ability of the Leaky Dielectric model to capture the behavior of the comb-drive actuator at submicron displacements does not come at the cost of micron scale performance. Overall, the Leaky Dielectric model achieves comparable, or better, tracking performance than both other models at all displacement scales and all concentrations tested. Above about 0.3 microns the error is always on the order of 10 percent, or less.

We end this section by exploring tracking error trends as a function of concentration. Figures 9a-9c shows errors at different concentrations for the three models. It is seen that, generally, both the Variable Resistor and Leaky Dielectric models decline in tracking performance with increasing concentration. The

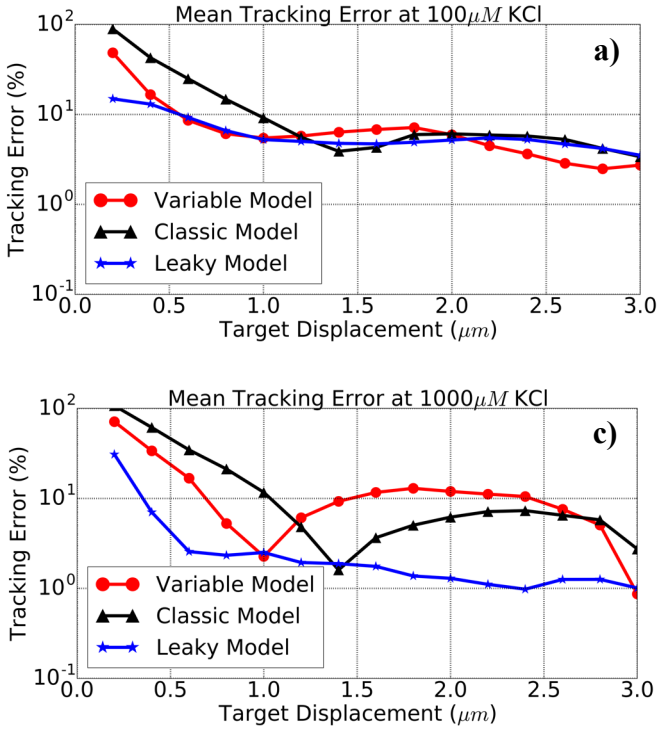

Fig 8: The mean tracking error for the Classic, Variable Resistor, and Leaky Dielectric circuit models, when they are fit to the data. The tracking error is shown at KCl concentrations of a) 100μM *,b)* 500μM *, and c)* 1000μM*. The tracking error is calculated as detailed in section VI.*

Leaky Dielectric model, however, appears to improve in tracking. This is a vital feature because some of the applications of the comb-drive actuator, especially those in the field of biology, require liquids with concentrations of electrolytes that are much greater than 100 μM.

VIII. CONCLUSION

We have constructed two novel models to describe the displacement of a comb-drive actuator in electrolytic liquids as a function of voltage and frequency. The Variable Resistor model accounts for the change in bulk electrolyte concentration as a function of time and the Leaky Dielectric model accounts for the fact that the native oxide is not a perfect dielectric. It is seen that the Leaky Dielectric model provides the greatest improvement in predicting the displacement of comb-drive actuators in electrolytes. It is also demonstrated that this Leaky Dielectric model has strong potential for use in open-loop and closed-loop control.

Further work is needed to improve and validate models for electrostatic actuation ionic media. We first need to test the ability of the Leaky Dielectric model to more accurately predict displacement at concentrations that accurately mimic biological media (order 100 mM). If the Leaky Dielectric model continues to perform well, robust open-loop and closed-loop control will be implemented using this model.

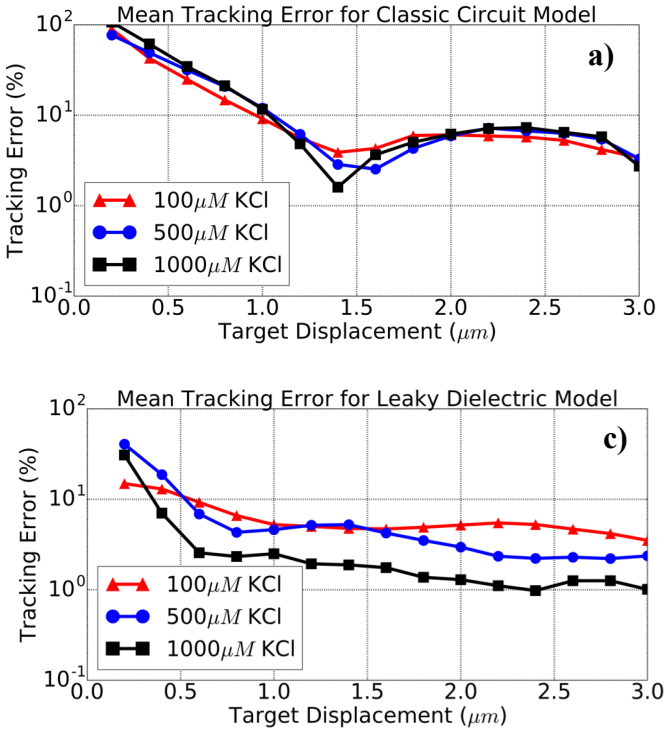

Fig 9: Plots that compare the mean tracking error at concentrations of 100μM, 500μM, *and* 1000μM *for the a) Classic Circuit, b) the Variable Resistor, and c)the Leaky Dielectric circuit models. The tracking error is calculated as detailed in section VI.*

ACKNOWLEDGEMENTS

The authors would like to acknowledge Ehsan Sadeghipour, Leeya Engel, and Gaspard Pardon for their invaluable contributions. The authors would also like to acknowledge financial support by a National Science Foundation Graduate Research Fellowship Grant no. DGE-4747 and a Stanford Graduate Fellowship.

This work was supported by the NSF within Stanford Nanofabrication Facility through the National Nanotechnology Infrastructure Network under Grant ECS-9731293.

REFERENCES

[1] T.L. Sounart, T.A. Michalske, and K.R. Zavadil. "Frequency-Dependent Electrostatic Actuation in Microfluidic MEMS," *Journal of Microelectromechanical Systems*, vol. 14, pp. 125-133, February 2005.

[2] V. Mukundan, P. Ponce, H. Butterfield, B.L. Pruitt, "Modeling and characterization of electrostatic comb-drive actuators in conducting liquid media," *Journal of Micromechanics and Microengineering*, 19 (9pp), 2009.

[3] H.V. Panchawagh, T.L. Sounart, R.L. Mahajan, "A Model for Electrostatic Actuation in Conducting Liquids," *Journal of Microelectromechanical Systems*, vol.18, pp. 1105-1117, October 2009.

APPENDIX A

The variable resistor system of ODEs is solved in dimensionless form. We first define:

$$\frac{dq}{dv} = C_0 = 2\epsilon = \frac{\lambda_D}{g} \tag{14}$$

$$\frac{dq}{dV_{EDL}} = \frac{dq}{dv} cosh\left(\frac{V_{EDL}}{2}\right) \tag{15}$$

where q is the surface charge density that gathers on the *EDL* capacitor, v is the dimensionless voltage, λ_D is the Debye length, and g is the gap length between two fingers on an electrode. Given this, the set of ODEs is as follows:

$$\frac{dq}{dt} = i \tag{16a}$$

$$\frac{dV_{EDL}}{dt} = \frac{dq}{dt} \Big/ \frac{dq}{dV_{EDL}} \tag{16b}$$

$$\frac{dV_{Stern}}{dt} = \frac{\varepsilon_{Stern}\lambda_D}{\varepsilon_{Water}\lambda_{Stern}} \frac{dq}{dv} \tag{16c}$$

$$\frac{di}{dt} = \frac{\left(\frac{dV_{Bulk}}{dt} - 2\frac{dV_{EDL}}{dt} - i\frac{dR_{Bulk}}{dt}\right)}{R_{Bulk}} \tag{16d}$$

$$\frac{dc_0}{dt} = -(2i)sgn(q) \tag{16e}$$

$$\frac{dR_{Bulk}}{dt} = \frac{-1}{2{c_0}^2}\frac{dc_0}{dt} \tag{16f}$$

$$\frac{dV_{Bulk}}{dt} = \frac{di}{dt}R_{Bulk} + i\frac{dR_{Bulk}}{dt} \tag{16g}$$

APPENDIX B

In this section, we briefly derive an expression for finding the displacement in the leaky dielectric model. Using basic impedance analysis, and building on work done in [2] and [3], we write

$$x = \varepsilon_r \alpha \left|\frac{Z_{Bulk}(\omega)}{Z_{System}(\omega)}\right| {V_{RMS}}^2 = \varepsilon_r \alpha h(\omega) {V_{RMS}}^2 \tag{17}$$

where

$$Z_{Bulk} = \frac{R_{Bulk}}{1 + j\omega R_{Bulk} C_{Bulk}} \tag{18}$$

and

$$Z_{System}(\omega) = Z_{Bulk} + 2Z_{OX}$$

APPENDIX C

Table 1

Model	Parameters Used for Fitting			
Classic	R_{Bulk}	τ_1	α	
Variable Resistor	R_{Ox}	C_{Ox}	τ_2	α
Leaky Dielectric	c_0	t_{Ox}	α	